Hybrid fluid-kinetic methods for space plasma simulation

Adam Stanier (Los Alamos National Laboratory)

International School/Symposium for Space Simulations (ISSS-15)
Max Planck Institute Plasma Physics, Garching, Germany

08/02/2024

LA-UR-24-27919

In this lecture

1. Motivating issue: scale separation in space plasma physics.

2. Introduction to hybrid fluid-kinetic methods.

3. Basic structure of a hybrid kinetic-ion fluid-electron PIC algorithm.

4. Numerical considerations to design and use a hybrid-PIC algorithm.

5. Applications of hybrid-PIC methods.

6. Fast particle kinetic hybrid model.

Slide 3

1. Scale separation in space plasma physics

Global MHD vs local kinetic (PIC/Vlasov) modeling

Kinetic Scales

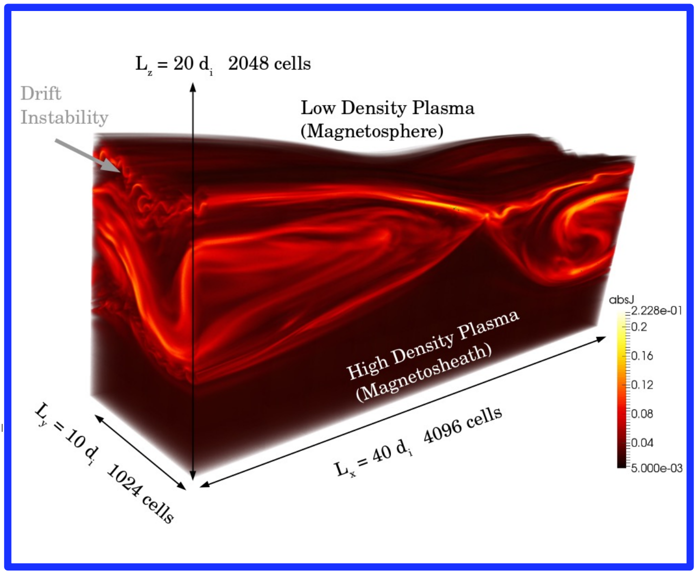

Macroscopic Scale

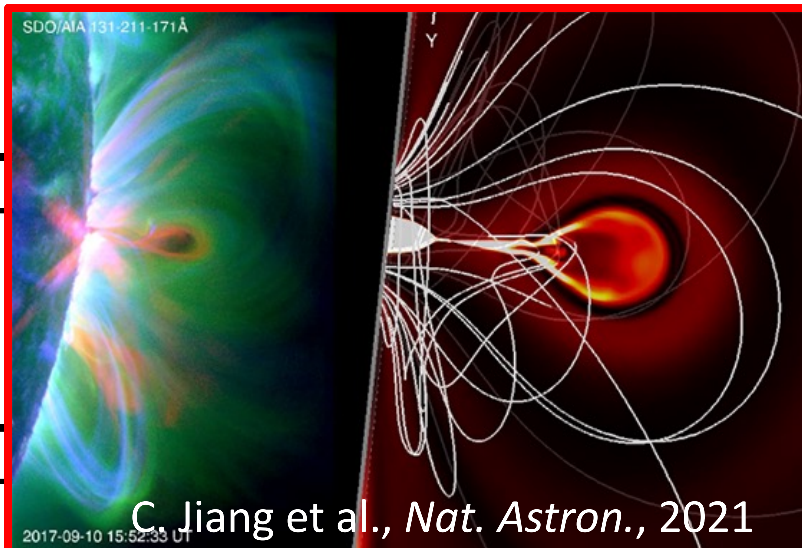

C. Jiang et al., *Nat. Astron.*, 2021

Fully Kinetic

MHD

Slide 5

Grand challenge: Modeling kinetic physics in global simulations

- **Key issues:**

1. Space plasma is virtually collisionless - invalidates MHD assumptions!
2. Kinetic PIC simulations good for studying local physics, but too expensive for global simulations.

These approaches miss potentially important coupling/feedback between different space plasma phenomena in a large global system.

E.g. shocks, reconnection, collisionless damping,…

2. Introduction to hybrid fluid-kinetic methods

Model reduction: The hybrid fluid-kinetic approach

- Choose to model:
  - Some part of the plasma kinetically (expensive).
  - Rest using a simplified fluid model (cheap).
- The choice here is problem dependent.
- Two common approaches
  - Kinetic ion + fluid electron: Suited to study coupling of large scale to ion scale behavior (trade electron scale accuracy for speed).
  - Plasma bulk fluid (MHD) + fast particle: Suited to study particle acceleration and transport by MHD-scale fluctuations.

Deriving the hybrid fluid-kinetic plasma model

1. Taking moments of the Vlasov for electrons:

Vlasov ions:

$$\partial_t f_i + \boldsymbol{\nabla} \cdot (f_i \boldsymbol{v}) + (q_i/m_i)(\boldsymbol{E} + \boldsymbol{v} \times \boldsymbol{B}) \cdot \boldsymbol{\nabla}_v f_i = 0.$$

Moment for electrons:

$$\partial_t n_e + \boldsymbol{\nabla} \cdot (n_e \boldsymbol{u}_e) = 0,$$

$$m_e n_e D_t (\boldsymbol{u}_e) + \boldsymbol{\nabla} \cdot \boxed{\mathbb{P}_e} + e n_e (\boldsymbol{E} + \boldsymbol{u}_e \times \boldsymbol{B}) = 0,$$

Pressure tensor

$$\vdots$$

Infinite # equations!

Electromagnetic fields:

$$c^{-2}\partial_t \boldsymbol{E} = \boldsymbol{\nabla} \times \boldsymbol{B} - \mu_0 \boldsymbol{j}, \qquad \partial_t \boldsymbol{B} = -\boldsymbol{\nabla} \times \boldsymbol{E},$$

$$\boldsymbol{\nabla} \cdot \boldsymbol{E} = \rho/\epsilon_0, \qquad \boldsymbol{\nabla} \cdot \boldsymbol{B} = 0.$$

- So far no approximations made.. (equivalent to Vlasov-Maxwell).

Deriving hybrid model: Simplifying assumptions

- Quasi-neutrality: Ion and electron charge densities are approximately equal: $\rho/en_e = (q_i n_i - en_e)/en_e \sim 0$.

  ➢ Hybrid model breaks down in vacuum regions!

- Non-relativistic ($c \to \infty, \quad \epsilon_0 \to 0$): Removes light waves from the model.

  ➢ These modify the Maxwell equations as:

  1. Gauss' law: $$\boldsymbol{\nabla} \cdot \boldsymbol{E} = \frac{q_i n_i - e n_e}{\epsilon_0} \to \frac{0}{0}!$$
  2. Maxwell-Ampere: $$\cancelto{0}{c^{-2}\partial_t \boldsymbol{E}} = \boldsymbol{\nabla} \times \boldsymbol{B} - \mu_0 \boldsymbol{j}$$

- How to we calculate electric field now? Electron momentum equation!

Deriving hybrid model: Simplifying assumptions

- Full Ohm's law:

$$\boldsymbol{E} = \underbrace{-\boldsymbol{u}_e \times \boldsymbol{B}}_{\underbrace{-\boldsymbol{u}_i \times \boldsymbol{B}}_{\text{Convective}} + \underbrace{\frac{\boldsymbol{j} \times \boldsymbol{B}}{en}}_{\text{Hall}}} - \overbrace{\frac{m_e D_t \boldsymbol{u}_e}{e}}^{\text{Inertial}} - \overbrace{\frac{\boldsymbol{\nabla} \cdot \mathbb{P}_e}{en}}^{\text{Pressure tensor}},$$

- At this point still have infinite moment equations ($\mathbb{P}_e$, etc): need closure!
- Many possible choices to truncate & simplify.
- Typically, we choose simply:
  - Isothermal electrons: $P_e \sim T_{e0}\, n$,
  - Adiabatic electrons: $P_e \sim T_{e0}\, n^{\gamma}$ with $\gamma=5/3$.
- Another common simplification is m_e -> 0 (remove electron kinetic scales).

Hybrid full-orbit ion and fluid electron model

- With all of the above assumptions we have:

Full-orbit ions: $$\partial_t f_i + \boldsymbol{\nabla} \cdot (f_i \boldsymbol{v}) + (q_i/m_i)(\boldsymbol{E} + \boldsymbol{v} \times \boldsymbol{B}) \cdot \boldsymbol{\nabla}_v f_i = 0.$$

Ohm's law: $$\boldsymbol{E} = -\boldsymbol{u}_i \times \boldsymbol{B} + \frac{\boldsymbol{j} \times \boldsymbol{B} - \boldsymbol{\nabla} p_e}{en},$$

Faraday: $$\partial_t \boldsymbol{B} = -\boldsymbol{\nabla} \times \boldsymbol{E},$$

Ampere: $$\boldsymbol{j} = (\boldsymbol{\nabla} \times \boldsymbol{B})/\mu_0,$$

Solenoidal: $$\boldsymbol{\nabla} \cdot \boldsymbol{B} = 0.$$

Adiabatic pressure: $$p_e = T_{e0} n_0 (n/n_0)^\gamma.$$

Closed via:

Quasi-neutrality: $$n = n_i = \frac{1}{e} \int q_i f_i d^3 v,$$

Ion current carrying velocity: $$\boldsymbol{u}_i = \frac{1}{en} \int q_s \boldsymbol{v} f_i d^3 v.$$

Los Alamos NATIONAL LABORATORY

Normalization: Ion units for EM hybrid model

- Take some reference parameters:
  - B_0 magnetic field, n_0 density, m_0 ion mass, v_0 velocity, L_0 distance, T_0 temperature.

- Write each variable $\chi = \boxed{\chi_0}\boxed{\hat{\chi}}.$ Normalized variable

  Reference value

➢ Ohm's law: $$\hat{\boldsymbol{E}} = -\hat{\boldsymbol{u}}_i \times \hat{\boldsymbol{B}} + \frac{\hat{d}_i}{\hat{n}}\left(\left(\hat{\boldsymbol{\nabla}} \times \hat{\boldsymbol{B}}\right) \times \hat{\boldsymbol{B}} - \hat{\boldsymbol{\nabla}}\hat{p}_e\right)$$

- Here $$\hat{d}_i = \frac{d_i}{L_0}, \quad \boxed{d_i = \frac{v_A}{\Omega_{ci}},} \quad \boxed{v_A = \frac{B_0}{\sqrt{\mu_0 n_0 m_0}},} \quad \boxed{\Omega_{ci}^{-1} = \frac{m_0}{eB_0}}$$

  Ion skin-depth (length) — Alfven speed (velocity) — Inverse gyro-freq (time)

- Drop '^' notation for normalized units. In these ion units $\hat{d}_i = 1.$

Los Alamos NATIONAL LABORATORY

Scale bridging via hybrid kinetic-ion fluid-electron model

Kinetic Scales

Macroscopic Scale

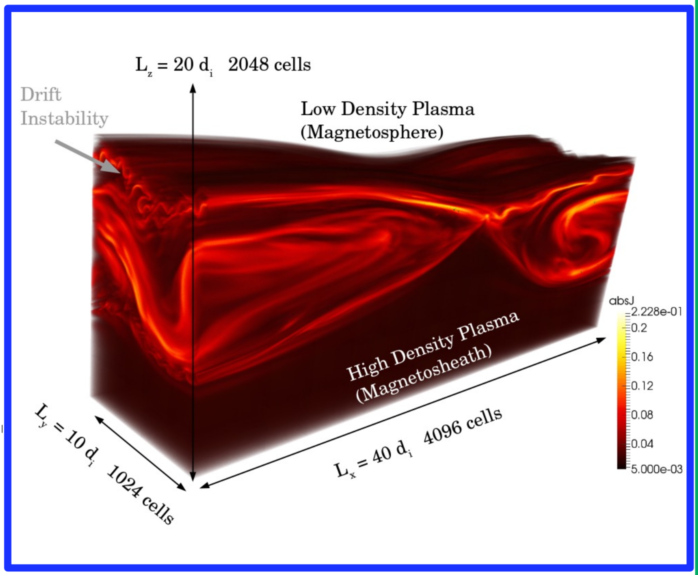

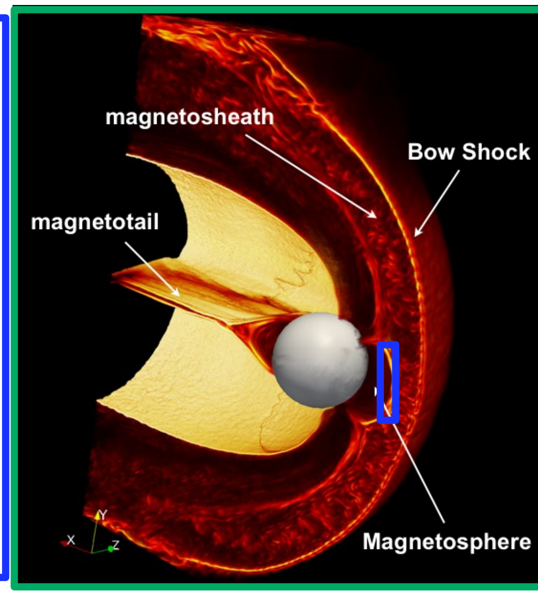

L

Spatial Scale

$$\tau_A = L/V_A$$

Time Scale

Fully Kinetic

MHD

Hybrid
(or Gyrokinetic, or Multi-Fluid)

Methods to solve the hybrid model equations

- Two main approaches to solve the hybrid model.

1. Continuum:
   - Discretize the 6D distribution function $f_i(\mathbf{x},\mathbf{v})$ on a spatial mesh.
   - Noise free, but can be have a large memory footprint (curse of dimensionality).

2. Hybrid particle-in-cell:
   - Ion distribution $f_i(\mathbf{x},\mathbf{v})$ represented by particles.
   - Subject to finite particle noise ~ 1/sqrt(N_p).

- I will focus on this second approach in this lecture:
  - Particle-In-Cell solution to the kinetic-ion fluid-electron plasma model.

3. Basic structure of a hybrid-PIC algorithm

Kinetic ions are discretized with marker particles

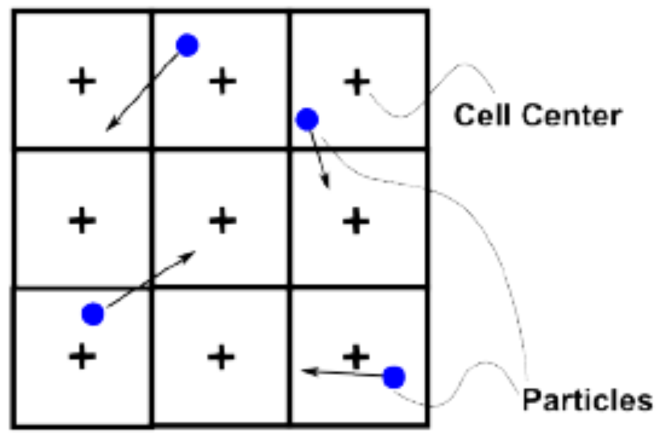

Grid for Computational Domain

- Vlasov equation:

$$\partial_t f_i + \boldsymbol{\nabla} \cdot (f_i \boldsymbol{v}) + (q_i/m_i)\left(\boldsymbol{E} + \boldsymbol{v} \times \boldsymbol{B}\right) \cdot \boldsymbol{\nabla}_v f_i = 0.$$

- Discrete sum of marker particles:

$$\boxed{f_i = \sum_p S\left[\boldsymbol{x} - \boldsymbol{x}_p(t)\right] \delta\left[\boldsymbol{v} - \boldsymbol{v}_p(t)\right]} \Rightarrow \begin{cases} \dfrac{d\boldsymbol{x}_p}{dt} = \boldsymbol{v}_p, \\ \dfrac{d\boldsymbol{v}_p}{dt} = \dfrac{q_i}{m_i}\left(\boldsymbol{E}_p + \boldsymbol{v}_p \times \boldsymbol{B}_p\right). \end{cases}$$

Finite-size in real space

Point-like in velocity space

Particle equations of motion: Time discretization

- Ions may gyrate >100-1000 times around the magnetic field within a simulation.
- Key requirements:
  - Long term orbit accuracy,
  - Preserve kinetic energy (gyroradius).
- Most used are variants of the *leapfrog* method.

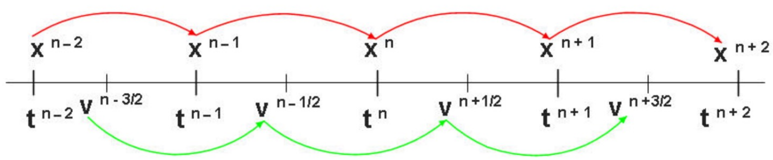

- Boris-push for velocity update:

Half-step with E: $$\boldsymbol{v}_p^- = \boldsymbol{v}_p^{n-1/2} + \frac{\Delta t}{2}\frac{q_p}{m_p}\boldsymbol{E}_p^n,$$

Rotation about B: $$\boldsymbol{v}_p^+ - \boldsymbol{v}_p^- = \Delta t \frac{q_p}{m_p}\left(\frac{\boldsymbol{v}_p^+ + \boldsymbol{v}_p^-}{2}\right) \times \boldsymbol{B}_p^n,$$

Half-step with E: $$\boldsymbol{v}_p^{n+1/2} = \boldsymbol{v}_p^+ + \frac{\Delta t}{2}\frac{q_p}{m_p}\boldsymbol{E}_p^n.$$

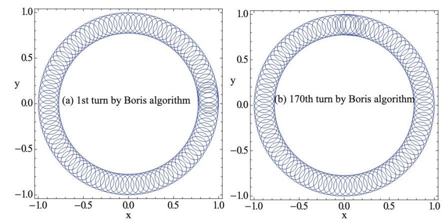

Figure 1: The Boris algorithm gives the correct orbit at the beginning (a) and later stage (b) of the numerical solution.

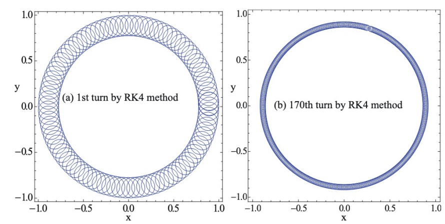

Figure 2: The RK4 method fails to generate the correct orbit at the later stage due to the accumulation of numerical error.

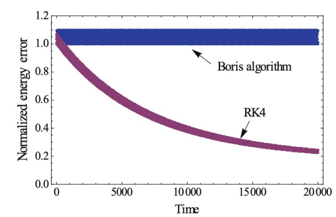

Figure 3: The energy error for the Boris algorithm is bounded for all time-steps, whiles that for the RK4 method increases without bound. The time axis has been normalized by the gyro-period.

Taken from Qin et al., "Why is the Boris algorithm so good?" *Phys. Plasmas* (2013)

Los Alamos NATIONAL LABORATORY

Mesh-based fluid electrons/EM fields

- Unlike typical MHD & PIC codes, most hybrid-PIC codes use a very simple cell-centered discretization:

$$\boxed{\begin{aligned} &\boldsymbol{E}_g = -\boldsymbol{u}_g \times \boldsymbol{B}_g + \frac{(\boldsymbol{\nabla} \times \boldsymbol{B}_g) \times \boldsymbol{B}_g - \boldsymbol{\nabla}(p_e)_g}{e n_g} = 0, \\ &\partial_t \boldsymbol{B}_g = -\boldsymbol{\nabla} \times \boldsymbol{E}_g. \end{aligned}}$$

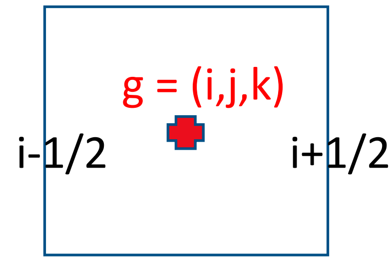

Where e.g. $\boldsymbol{\nabla}\chi_g = \dfrac{\chi_{i+1,j,k} - \chi_{i-1,j,k}}{2\Delta x}\hat{\boldsymbol{x}} + \ldots$

- Centered discretization of advection terms can be unstable!
  - ➢ But in hybrid advection is handled by particles!
- Cell centered does conserve $\boldsymbol{\nabla} \cdot \boldsymbol{B}_g = 0.$
- Explicit time-stepping for hybrid is much more complicated! – in a few slides.

Particle-Mesh interpolation

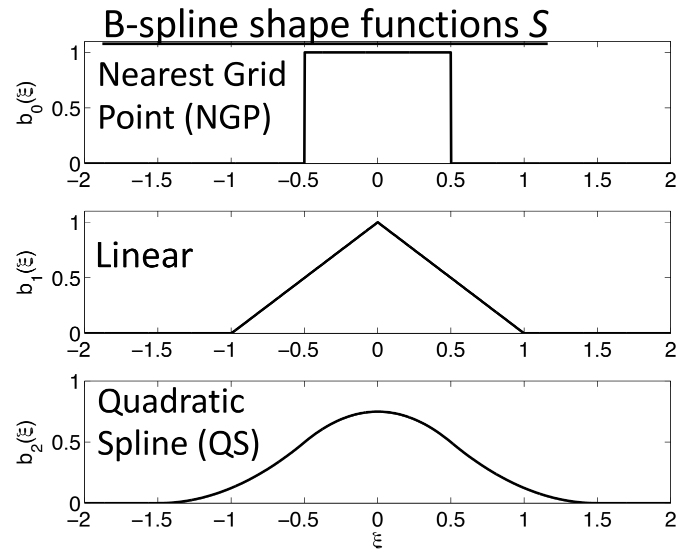

- Scatter fields: $\boldsymbol{E}_p = \sum_g S(\boldsymbol{x}_g - \boldsymbol{x}_p)\boldsymbol{E}_g,$

$$\boldsymbol{B}_p = \sum_g S(\boldsymbol{x}_g - \boldsymbol{x}_p)\boldsymbol{B}_g$$

- Gather moments: $n_g = \frac{1}{e}\sum_p q_p S(\boldsymbol{x}_g - \boldsymbol{x}_p)/\Delta V,$

$$\boldsymbol{u}_g = \frac{1}{e n_g}\sum_p q_p \boldsymbol{v}_p S(\boldsymbol{x}_g - \boldsymbol{x}_p)/\Delta V$$

- PIC codes often spend most runtime doing these particle-mesh interpolations!
- Higher order shape functions reduce noise, but more expensive.
- Extra care needs to be used with higher order shape functions in hybrid-PIC due to the *hybrid cancellation problem*! (see later).

Additional spatial smoothing

- In my experience, hybrid-PIC seems to be more noisy than regular Vlasov-Maxwell PIC.
- No proof of this statement at present, but consider:

$$p_e = T_{e0} n_0 (n/n_0)^\gamma . \qquad \boldsymbol{E} = -\boldsymbol{u}_i \times \boldsymbol{B} + \frac{\boldsymbol{j} \times \boldsymbol{B} - \boldsymbol{\nabla} p_e}{en},$$

Noisy (from particles)

Gradient of noisy quantity amplifies noise

➢ Smoothing often used in hybrid-PIC.

Quick and effective:

Binomial filter ‘SM’: $\frac{1}{4}\begin{bmatrix}1\\2\\1\end{bmatrix} * \frac{1}{4}\begin{bmatrix}1 & 2 & 1\end{bmatrix} \longrightarrow \frac{1}{16}\begin{bmatrix}1 & 2 & 1\\2 & 4 & 2\\1 & 2 & 1\end{bmatrix}$

Smooth moments: $n_g \to \mathrm{SM}(n_g), \quad \boldsymbol{u}_g \to \mathrm{SM}((n\boldsymbol{u})_g)/\mathrm{SM}(n_g),$

& smooth fields: $\boldsymbol{E}_p^* = \sum_g S(\boldsymbol{x}_g - \boldsymbol{x}_p)\,\mathrm{SM}(\boldsymbol{E}_g^*), \quad \boldsymbol{B}_p = \sum_g S(\boldsymbol{x}_g - \boldsymbol{x}_p)\,\mathrm{SM}(\boldsymbol{B}_g).$

4. Numerical considerations to design and use a hybrid-PIC algorithm

To compare: Explicit time-stepping in Vlasov-Maxwell PIC

- In Vlasov-Maxwell PIC, explicit time-stepping fits together well:
- Assume we know: $\boldsymbol{v}_p^{n-1/2},\ \boldsymbol{x}_p^n,\ \boldsymbol{B}^n,\ \boldsymbol{E}^n$

Staggered to leapfrog

Leap-frog particles (second order, Volume preserving)

$$
\left\{
\begin{aligned}
\boldsymbol{v}_p^{n+1/2} &= \boldsymbol{v}_p^{n-1/2} + \Delta t \left[\boldsymbol{E}_p^n + \frac{\left(\boldsymbol{v}_p^{n+1/2} + \boldsymbol{v}_p^{n-1/2}\right)}{2} \times \boldsymbol{B}^n \right], \\
\boldsymbol{x}_p^{n+1} &= \boldsymbol{x}_p^n + \Delta t\, \boldsymbol{v}_p^{n+1/2}.
\end{aligned}
\right.
$$

Verlet fields (leapfrog)

$$
\left\{
\begin{aligned}
\boldsymbol{B}^{n+1/2} &= \boldsymbol{B}^n - (\Delta t/2)\, \boldsymbol{\nabla} \times \boldsymbol{E}^n, \\
\boldsymbol{E}^{n+1} &= \boldsymbol{E}^n + \Delta t \left[\boldsymbol{\nabla} \times \boldsymbol{B}^{n+1/2} - \boldsymbol{j}^{n+1/2} \right], \\
\boldsymbol{B}^{n+1} &= \boldsymbol{B}^{n+1/2} - (\Delta t/2) \boldsymbol{\nabla} \times \boldsymbol{E}^{n+1}.
\end{aligned}
\right.
$$

Los Alamos NATIONAL LABORATORY

Can we take the same approach in hybrid-PIC?

- Assume known ($\boldsymbol{v}_p^{n-1/2}$, $\boldsymbol{x}_p^n$, $\boldsymbol{B}^n$, $\boldsymbol{E}^n$), then

Explicit Boris push (second order, Volume preserving)

$$\begin{cases} \boldsymbol{v}_p^{n+1/2} = \boldsymbol{v}_p^{n-1/2} + \Delta t \left[\boldsymbol{E}_p^n + \dfrac{\left(\boldsymbol{v}_p^{n+1/2} + \boldsymbol{v}_p^{n-1/2}\right)}{2} \times \boldsymbol{B}^n \right], \\ \boldsymbol{x}_p^{n+1} = \boldsymbol{x}_p^n + \Delta t\, \boldsymbol{v}_p^{n+1/2}. \end{cases}$$

Static Ohm's law:

$$\left.\begin{aligned} \boldsymbol{B}^{n+1/2} &= \boldsymbol{B}^n - (\Delta t/2)\, \boldsymbol{\nabla} \times \boldsymbol{E}^n, \\ &\boxed{\boldsymbol{E}^{n+1/2} = -\boldsymbol{u}^{n+1/2} \times \boldsymbol{B}^{n+1/2} + \ldots} \\ \boldsymbol{B}^{n+1} &= \boldsymbol{B}^n - \Delta t \boldsymbol{\nabla} \times \boldsymbol{E}^{n+1/2}. \end{aligned}\right\}$$

Explicit midpoint (second order)

Lastly:

$$\boxed{\boldsymbol{E}^{n+1} = -\boxed{\boldsymbol{u}^{n+1}} \times \boldsymbol{B}^{n+1} + \ldots}$$

<u>Unknown</u>! We have implicit coupling $\boldsymbol{E}^{n+1} = \boldsymbol{E}^{n+1}\left(\boldsymbol{v}_p^{n+3/2}\left(\boldsymbol{E}^{n+1}\right)\right).$

Explicit hybrid-PIC time-stepping schemes

- This has been dealt with (explicitly) via:
  1. Velocity moment extrapolation:

$$\boldsymbol{u}^{n+1} = \frac{3}{2}\boldsymbol{u}^{n+1/2} - \frac{1}{2}\boldsymbol{u}^{n-1/2}.$$

  2. Predictor-corrector methods:

Predict:
$$\begin{cases} \boldsymbol{E}'^{\,n+1} = 2\boldsymbol{E}^{n+1/2} - \boldsymbol{E}^{n}, \\ \boldsymbol{E}'^{\,n+1} \xrightarrow{\text{push}} v_p'^{\,n+3/2} \xrightarrow{\text{Faraday/Ohm}} (\boldsymbol{B}, \boldsymbol{E}')^{n+3/2}, \end{cases}$$

Correct:
$$\boldsymbol{E}^{n+1} = \frac{1}{2}\left(\boldsymbol{E}'^{\,n+3/2} + \boldsymbol{E}^{n+1/2}\right).$$

  3. Moment methods:

$$(n\boldsymbol{u})^{n+1} = (n\boldsymbol{u})^{n+1/2} + \frac{e\Delta t}{2m}\left[n^{n+1/2}\boldsymbol{E}^{n+1/2} + (n\boldsymbol{u})^{n+1/2} \times \boldsymbol{B}^{n+1/2}\right]$$

- See ISSS-series books by Winske et al.: (1991, 2003, 2022/2023?)

arXiv:2204.01676

Modern predictor^2-corrector scheme

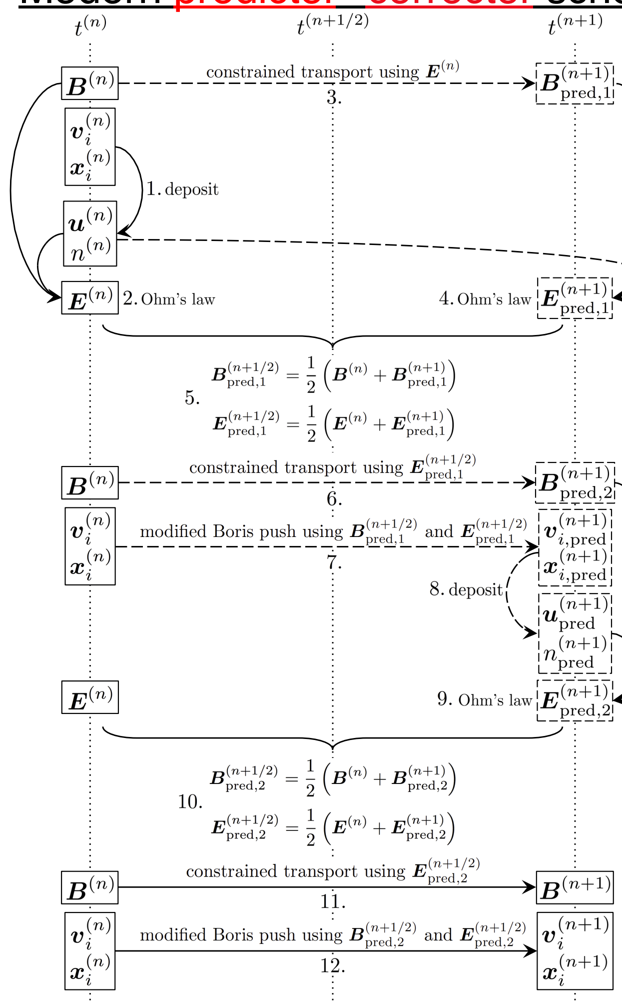

(Kunz et al., JCP 259, 154 (2014))

Time-stepping: Whistler wave dispersion

- Inclusion of Hall-term gives extremely stiff waves:

$$\frac{\partial \boldsymbol{B}}{\partial t} = -\boldsymbol{\nabla} \times \left(\frac{d_i}{n} \left(\boldsymbol{j} \times \boldsymbol{B} \right) \right) \quad \longrightarrow \quad \omega = i d_i v_A k^2$$

Quadratic dispersion

- This sets stiff CFL:

$$k_{\mathrm{max}} \sim \frac{1}{\Delta x} \quad \longrightarrow \quad \Delta t_{\mathrm{CFL}} \sim n \left(\Delta x \right)^2 / B$$

  - Usually shows up first as numerical instabilities in near vacuum regions.
  - Potential solutions:
    1. Sub-cycling,
    2. Electron inertia,
    3. Re-introduce speed of light,
    4. Implicit time-stepping.

Implicit time-stepping in hybrid-PIC methods

- Early efforts: implicit field solve (e.g. Hewett, 1980).
- More recently, fully implicit methods have been developed:
  1. Implicit scheme for electrostatic δF model (Sturdevant et al., J. Comp. Phys. 2016)
  2. Implicit scheme for electromagnetic full-F (Stanier et al., J. Comp. Phys. 2019).
     - Can take steps much larger than whistler Δt_{CFL}.
     - Exact conservation of momentum & energy.
     - Build on recent breakthroughs in implicit PIC methods (Markidis et al. J.Comp. Phys. 2011; Chen & Chacon J. Comp. Phys. 2011).

Numerical stability and dissipation

- Although space plasmas are close to collisionless, nonlinear numerical simulations typically need some dissipation for stability. Either via:

  1. Explicit terms in equations ("physical dissipation").
  2. Upwinding of advective terms (implicit dissipation via discretization).

- Hybrid models usually follow 1) by adding **dissipation in Ohm's law**:

$$\boldsymbol{E} = \underbrace{\boldsymbol{E}^*}_{\text{Frictionless E}} + \underbrace{\eta \boldsymbol{j}}_{\text{resistivity}} - \underbrace{\eta_H \nabla^2 \boldsymbol{j}}_{\text{"Hyper-resistivity"}}$$

Los Alamos NATIONAL LABORATORY

Hyper-resistivity: Why and what?

- Why? Hall-term is badly behaved!
- Consider damped Whistler dispersion:

1) Resistive 2) Hyper 3)Hall

$$\boxed{\omega = -ik^2\eta - ik^4\eta_H \pm d_i v_A k_{\parallel} k.}$$

a) Balance 1 & 3: Both ~ k^2 - Can't set a dissipation scale – Whistler noise!

b) Balance 2 & 3:

$$\boxed{\lambda = \frac{2\pi}{k} = 2\pi\sqrt{\frac{\eta_H}{d_i v_A}}}$$

➢ Want to set $\lambda \sim \Delta x$ to avoid whistler noise.

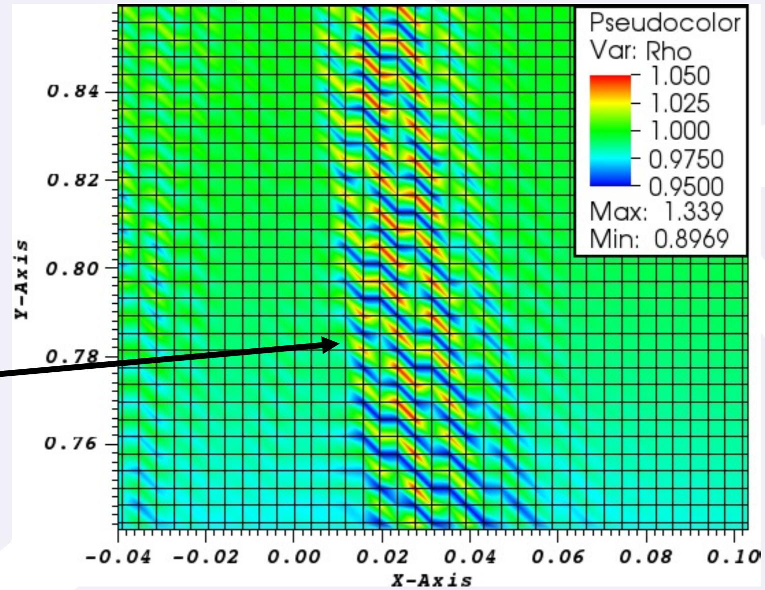

See e.g. Stanier, A., PhD Thesis (2013)

- What?
  - Similar form of an electron collisional viscosity: $\approx -\eta_H \nabla^2 \boldsymbol{u}_e$
  - But coefficient too large for space! Sometimes argued as "anomalous viscosity".

Conservation when including frictional terms

1. Momentum conservation:

- Collisionless Vlasov: $\partial_t f_i + \boldsymbol{\nabla} \cdot (f_i \boldsymbol{v}) + (q_i/m_i) \left(\boxed{\boldsymbol{E}^*} + \boldsymbol{v} \times \boldsymbol{B}\right) \cdot \boldsymbol{\nabla}_v f_i = 0.$
- Collisional Ohms: $\boldsymbol{E} = \boxed{\boldsymbol{E}^*} + \eta \boldsymbol{j} - \eta_H \nabla^2 \boldsymbol{j}$

➢ Total momentum conservation: Push with E*.

2. Energy conservation:

- Requires separate electron pressure equation with heating terms:

$$(\gamma - 1)^{-1} \left[\partial_t p_e + \boldsymbol{\nabla} \cdot (\boldsymbol{u}_e p_e)\right] + p_e \boldsymbol{\nabla} \cdot \boldsymbol{u}_e = \boxed{H_e} - \boldsymbol{\nabla} \cdot \boldsymbol{q}_e.$$

Frictional heating: $H_e = \eta j^2 + \eta_H \boldsymbol{\nabla} \boldsymbol{j} : \boldsymbol{\nabla} \boldsymbol{j}$

Finite grid instabilities for cold ions

Nearest Grid Point, no smooth, U_0/C_s = 0.1.

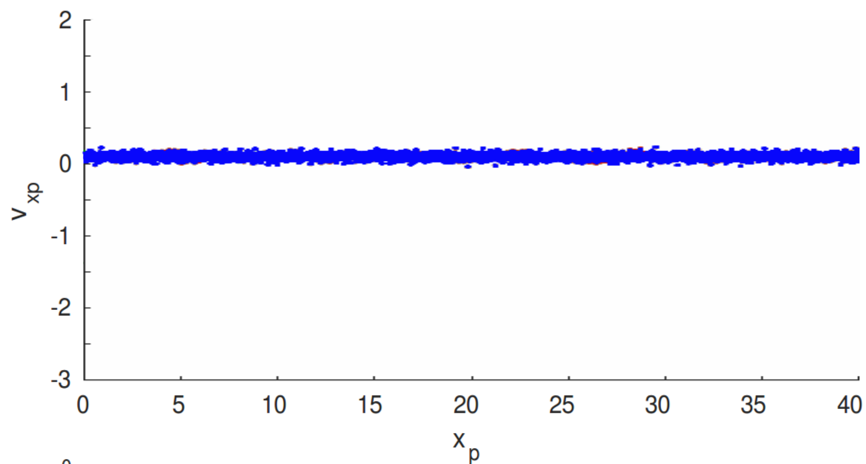

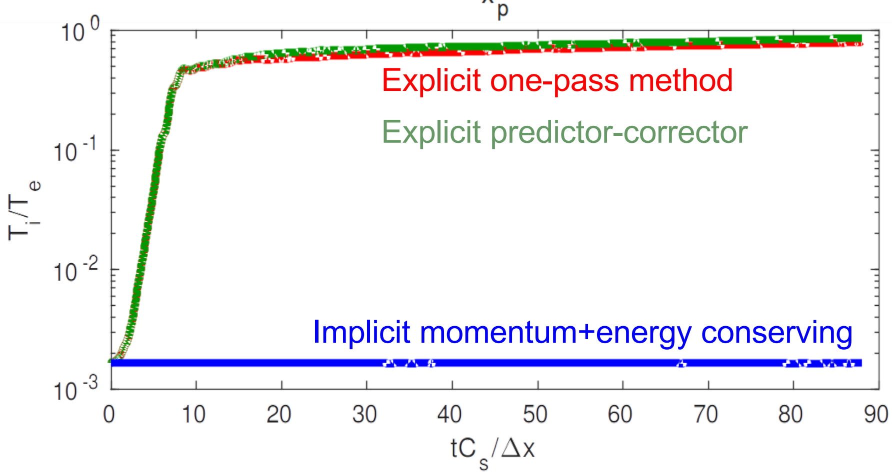

- Problem set-up: Cold ion beam moving through uniform spatial mesh.
- Non-conservative (explicit) schemes unstable for T_i/T_e << 1 regardless of spatial resolution (Rambo, J. Comput. Phys. 1995).
  - Precise threshold in T_i/T_e and beam velocity depends on shape-function.
  - NGP threshold >> QS threshold.
- Cause unstable (exponential) heating of ions until some saturation value & also violates momentum conservation.
- Implict momentum+energy conserving scheme stable w.r.t. these instabilities.

(Stanier et al., J. Comp. Phys. 2019)

Stochastic heating when FGI stable

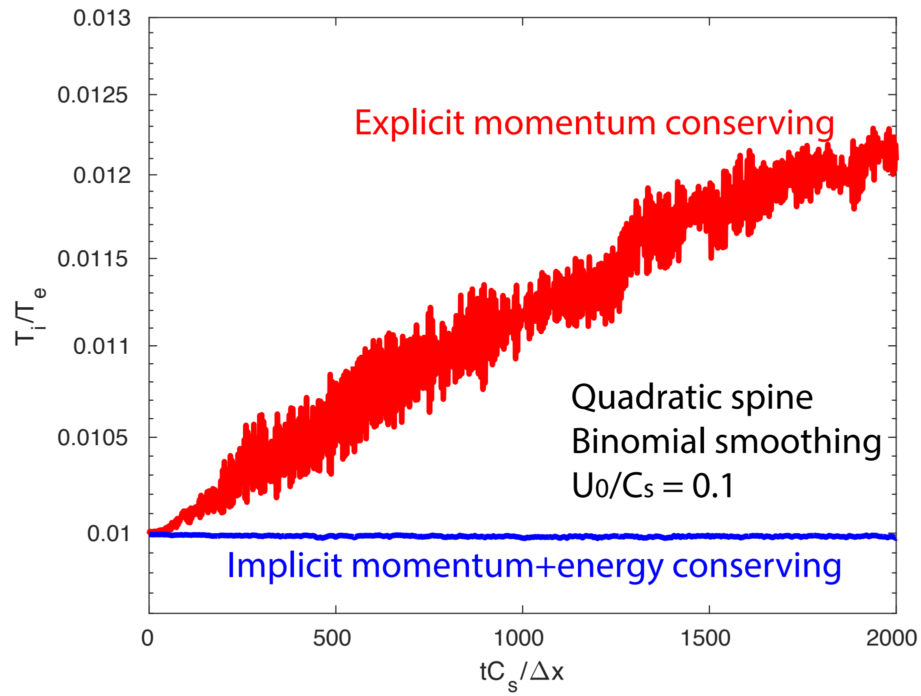

- For quadratic spline with smoothing, explicit becomes FGI stable for Ti/Te=0.01.
- However, significant stochastic heating for explicit (Rambo, JCP 97).
- Implicit scheme gives large improvement.

Slide 32

Minimum mesh resolution requirements

- "Hybrid cancellation problem" due to different discretization of ions (particles) and electrons (fluid). *Stanier et al., JCP 420,* 109705 *(2020)*
  - ➢ The error depends on shape function & amount of smoothing.

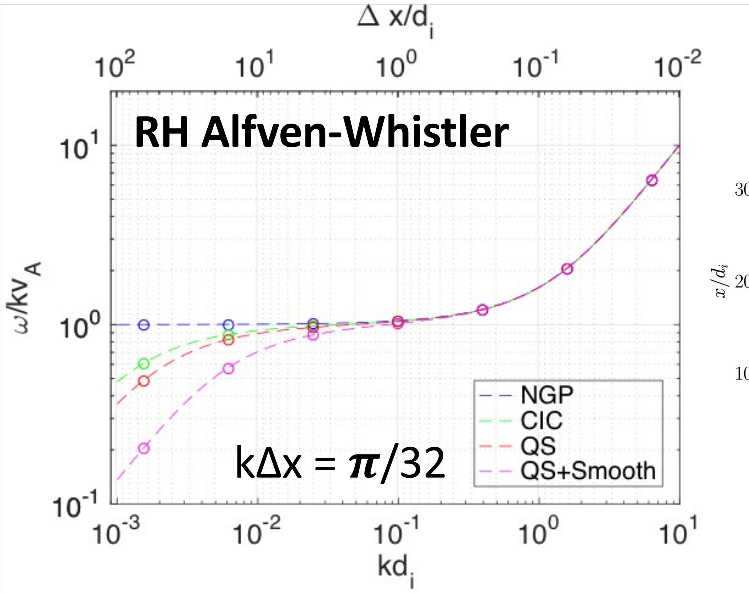

1D collisionless EM perpendicular shock generated by M_A=5 piston ions.

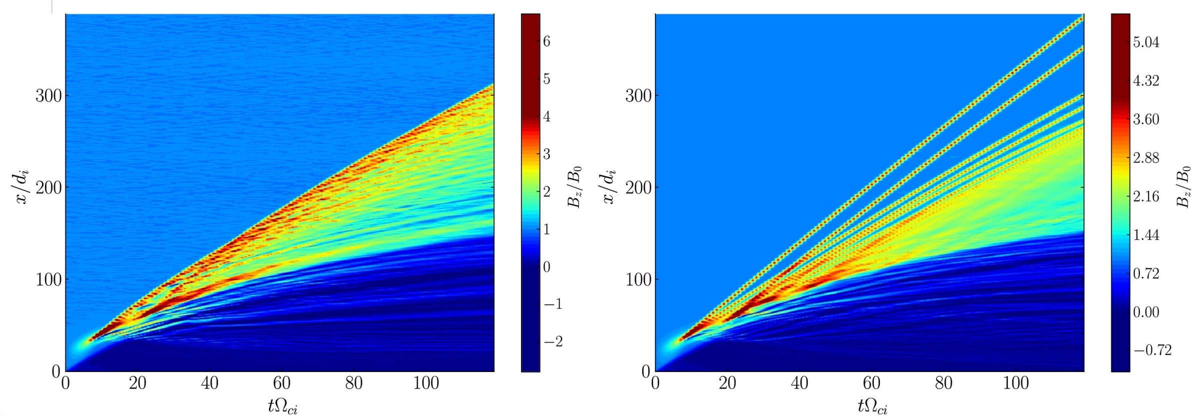

(a) Nearest Grid Point (NGP). $\Delta x/d_i = 1$.

(b) Quadratic Spline (QS) with smoothing. $\Delta x/d_i = 1$.

- NGP & no smoothing: can take Δx >> di (provided features resolved).
- In other cases: Need to resolve ion skin-depth (Δx/di < 1).

Los Alamos NATIONAL LABORATORY

5. Applications of hybrid-PIC methods

Macro- to ion-scale coupling is important in reconnection

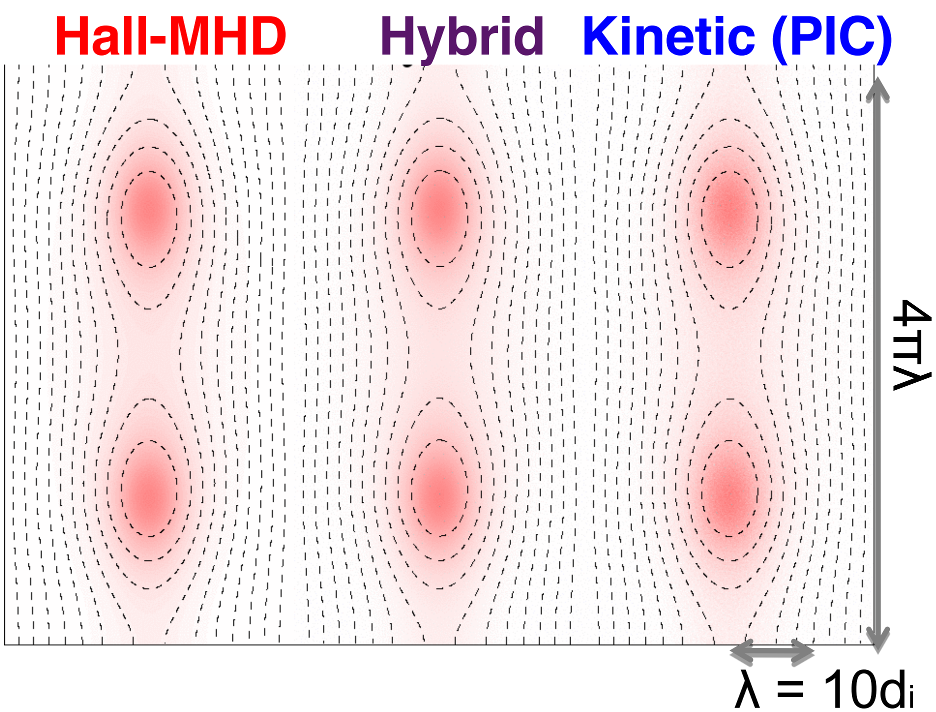

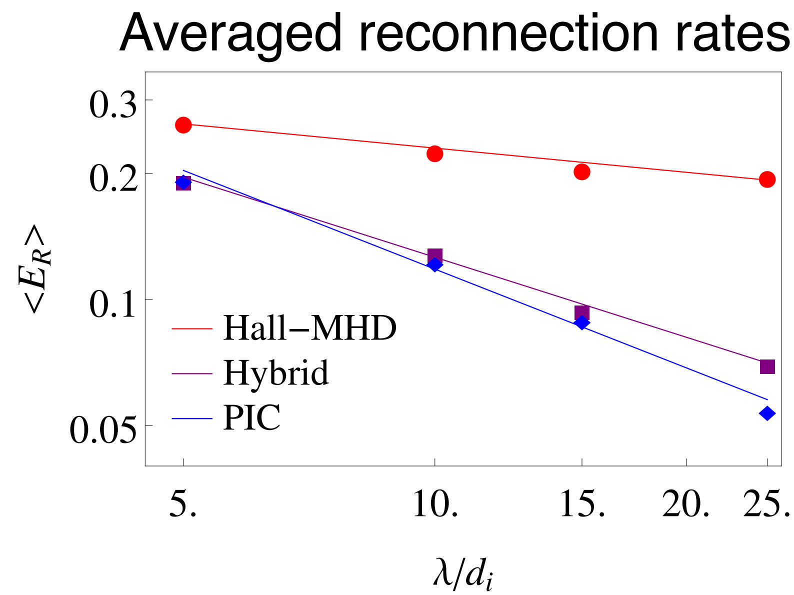

- **Hybrid** model minimum sufficient model to reproduce fully kinetic reconnection rates and macro-to-ion scale coupling (Stanier et al., PRL 2015, Ng et al., PoP 2016).
- Key ion kinetic physics missing from Hall-MHD fluid model.

Slide 35

Kinetic ion codes have different global behavior

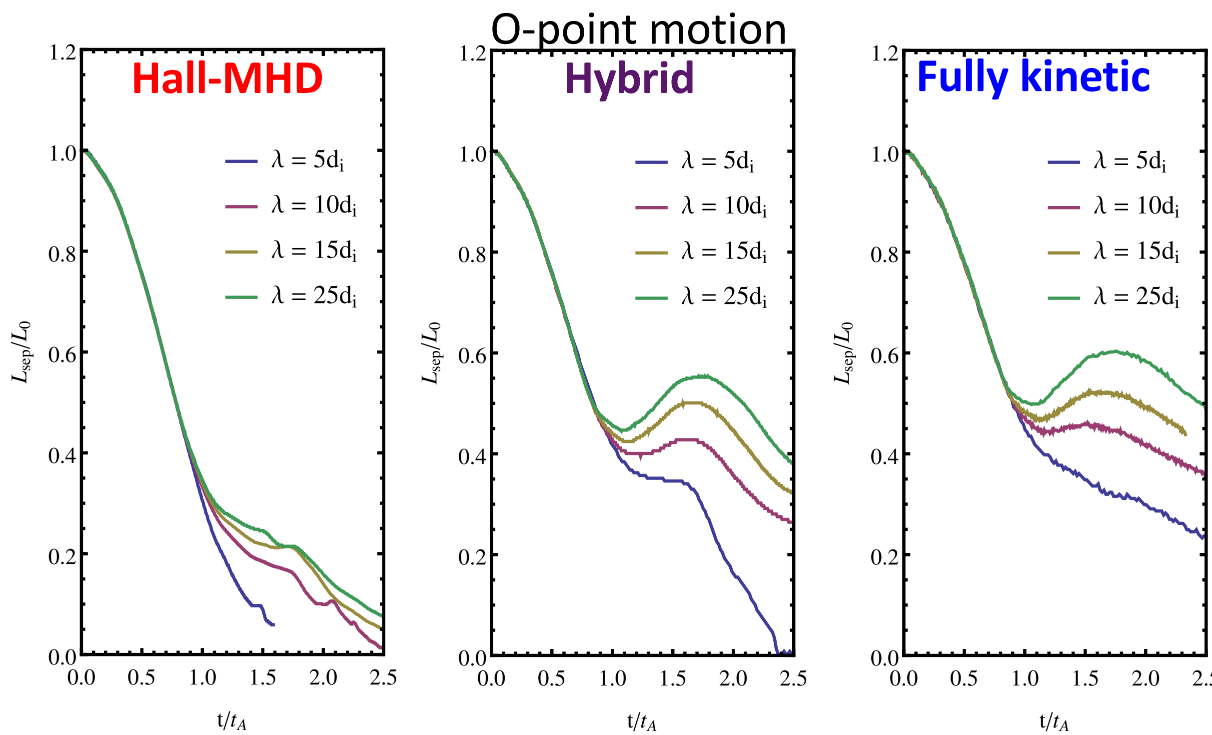

- Hybrid & fully kinetic: O-point reversal (sloshing) for $\lambda \geq 10\ d_i$.
- Hall-MHD: No clear reversal for $\lambda \leq 25\ d_i$.
- <u>Missing kinetic ion physics gives different global evolution.</u>

Los Alamos NATIONAL LABORATORY

Comparison with Hall-MHD

- Now if we similarly take moments of ion-Vlasov:

- 0th Continuity: $\partial_t n + \boldsymbol{\nabla} \cdot (n\boldsymbol{u}_i) = 0,$
- 1st (i+e) momentum:

$$\partial_t (mn\boldsymbol{u}_i) + \boldsymbol{\nabla} \cdot \left[mn\boldsymbol{u}_i\boldsymbol{u}_i - \boldsymbol{BB}/\mu_0 + \mathbb{I}(B^2/2\mu_0) + \overline{\overline{\boldsymbol{P}}} \right] = \boldsymbol{0}.$$

Hall-MHD (constant T_{i0}/T_{e0})

$$\overline{\overline{\boldsymbol{P}}} = p_e (1 + T_{i0}/T_{e0}) \mathbb{I}$$

Hybrid (single ion species)

$$\overline{\overline{\boldsymbol{P}}} = p_e \mathbb{I} + \int m_i f_i \boldsymbol{ww} d^3 w$$

- Hall-MHD is a “cold-ion” model in the sense that it does not include ion finite Larmor radius (FLR) or other kinetic effects from warm distribution functions.

Los Alamos NATIONAL LABORATORY

Missing physics: Finite ion-orbit effects

$$E'_z = (\boldsymbol{E} + \boldsymbol{v}_i \times \boldsymbol{B}) \cdot \hat{\boldsymbol{z}} =$$
$$\frac{d_i}{n}\left[\partial_t(n v_{iz}) + \boldsymbol{\nabla}\cdot(n\boldsymbol{v}_i v_{iz})\right] + \frac{d_i}{n}\boldsymbol{\nabla}\cdot\boldsymbol{P}_{iz} + F_{\mathrm{coll,z}}$$

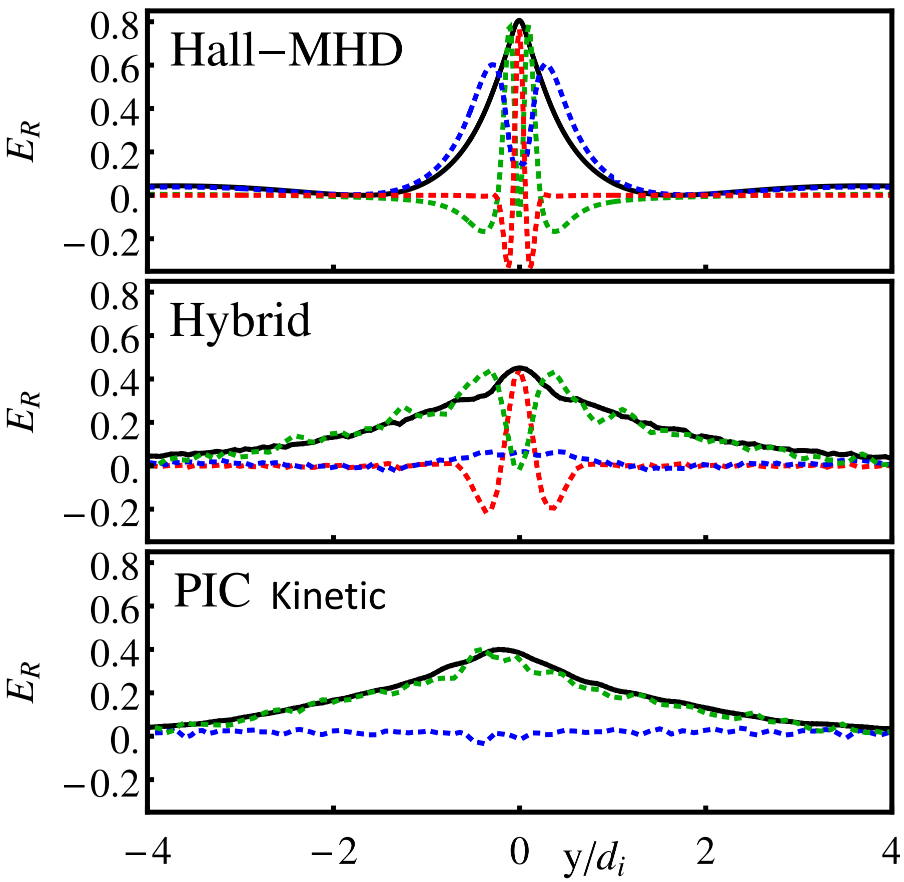

- Hybrid & fully kinetic:
  - Broader ion diffusion region.
  - Supported by non-gyrotropic $\underline{\mathbf{P}}_i$.
  - Set by meandering-type orbits (Speiser 1965).

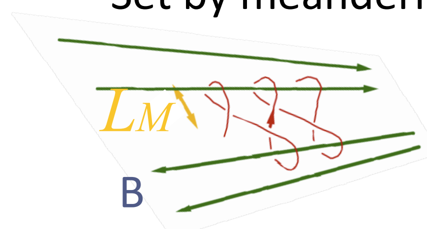

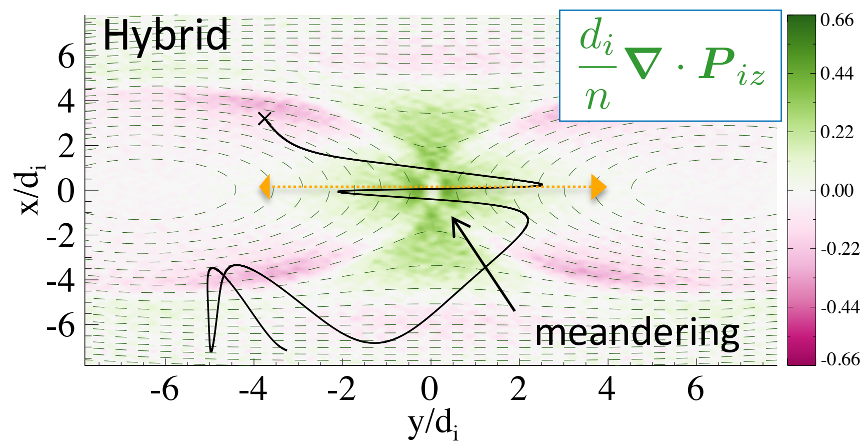

Proton Cyclotron Anisotropy Instability

- **Electromagnetic & multi-ion verification test:**
  - 1D-3V electromagnetic instability driven by $p_{i\perp}/p_{i//} > 1$.
  - Maximum growth at **kxB=0**, finite real frequency.
  - $k_x\Delta x = 0.065$, 50000 particles/cell, 2x binomial smooth, quiet start.

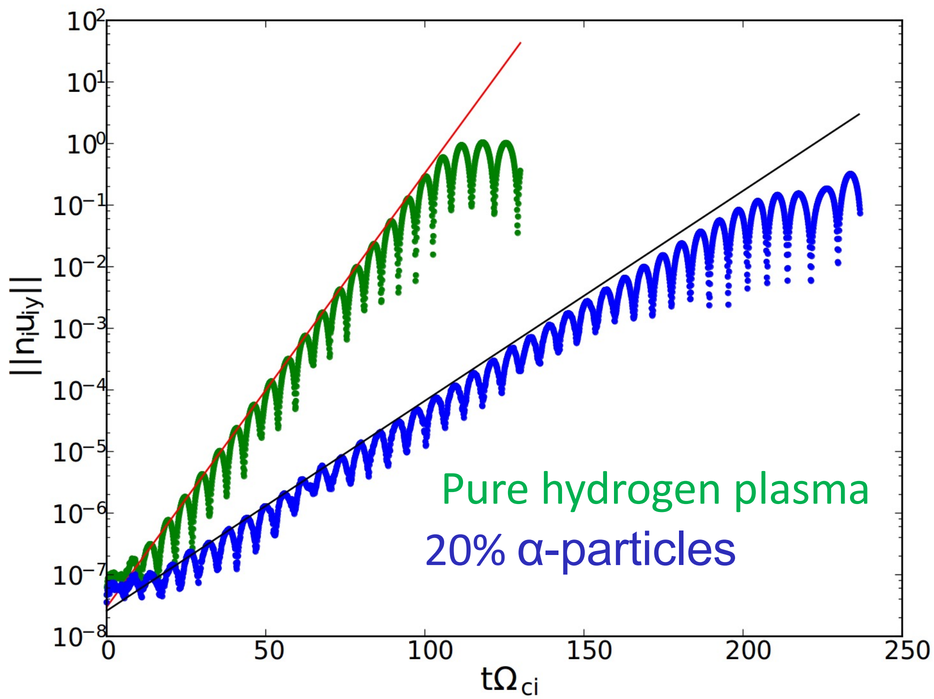

$p_{\alpha\perp}/p_{\alpha//} = p_{p\perp}/p_{p//} = 3$, $\beta_{p//} = 1$, $T_{\alpha//}/T_{p//} = 2$, $k_{//}d_p = 0.6$

Mercury

Results from Ari Le and Chuanfei Dong

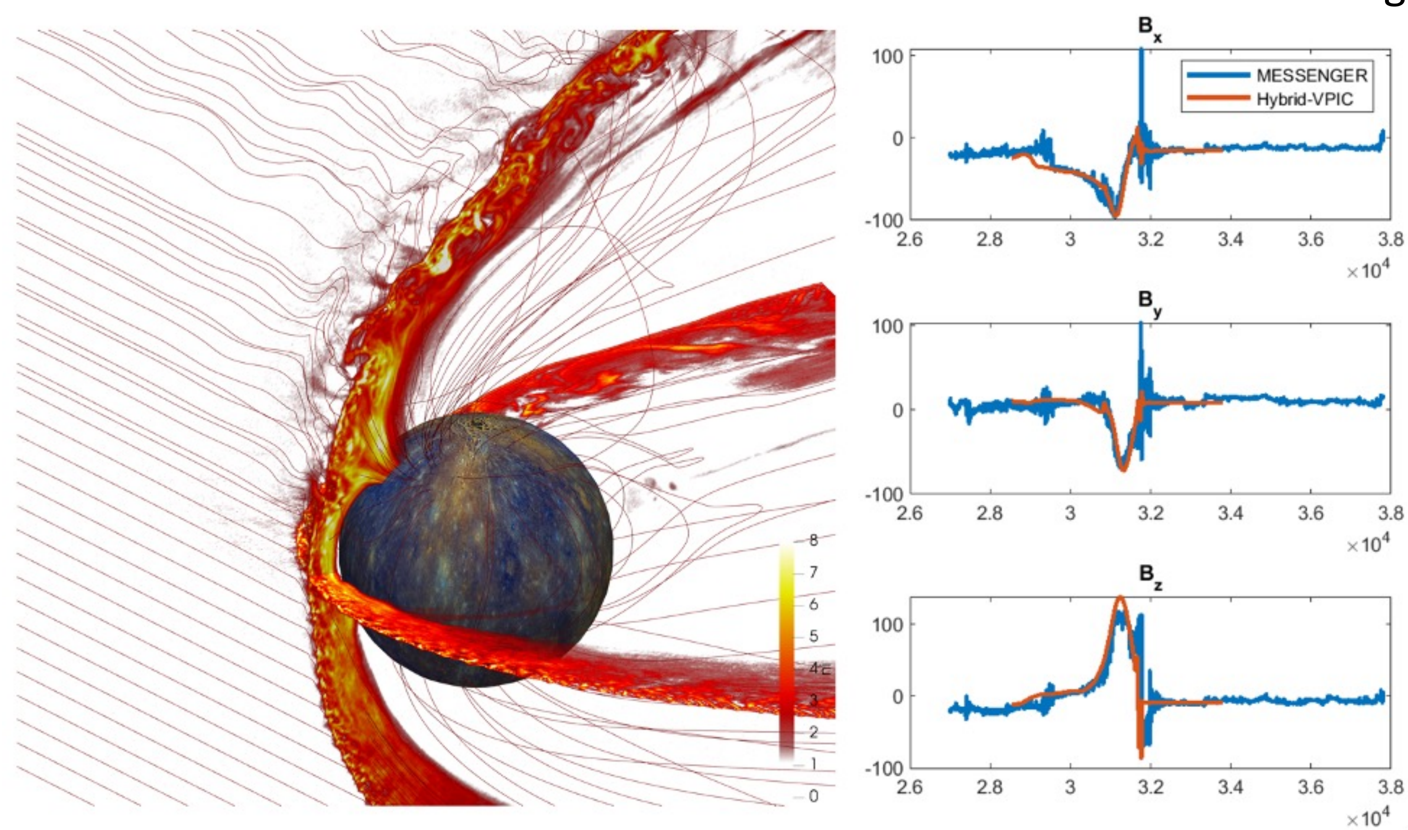

- 3D global hybrid simulations of Mercury (using hybridVPIC).
- Comparison with MESSENGER M2 flyby.
- Formation of ion foreshock in quasi-parallel region.

Earth-scale simulations (2D&3D)

2D run with domain size 8192x8192 d_i

Many islands in turbulent magnetosheath

Waves in ion foreshock

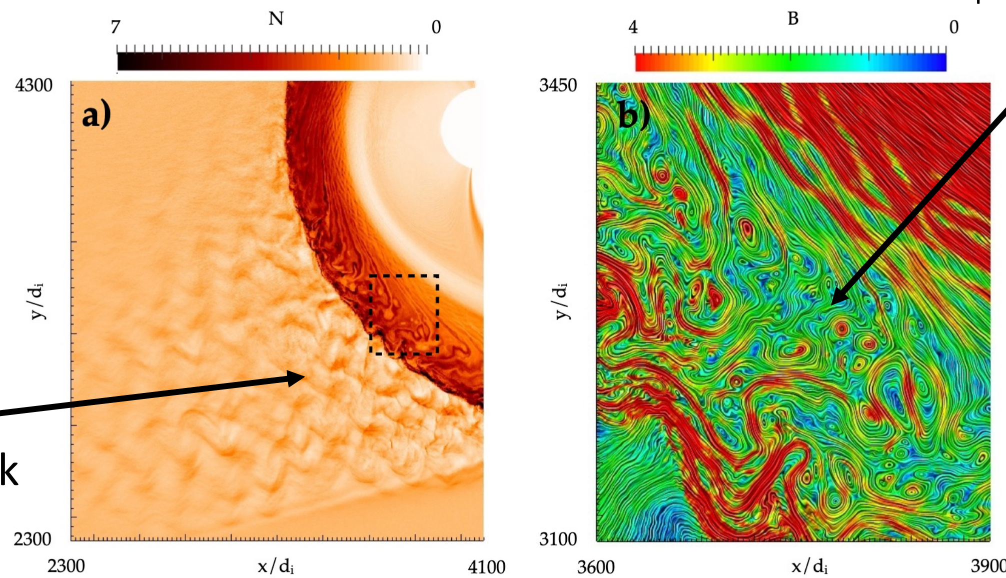

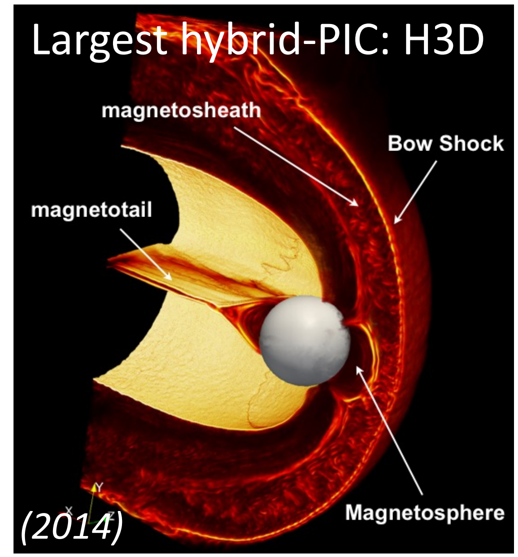

Fig. 4. Foreshock and magnetosheath turbulence in a 2D hybrid simulation describing interaction of solar wind injected from the left boundary with a dipolar field. Left: ion density; Right: LIC visualization of the magnetic field structure in a sub-region marked on the left panel. The scales are normalized to the ion inertial length d_i.

- (Karimabadi et al., Phys. Plasmas 2014): “The links between shocks, reconnection and turbulence”.

Los Alamos NATIONAL LABORATORY

6. Fast particle kinetic hybrid model

Fast-particle hybrid models

- Have greater use in magnetic fusion and astrophysics (cosmic rays) applications.
- Some recent interest to develop new models to solar particle acceleration (Drake et al. Phys. Plasmas 2019).
- MHD + fast particle using current-coupling:

$$
\left\{
\begin{array}{l}
\partial_t n + \boldsymbol{\nabla}\cdot(n\boldsymbol{U}) = 0,\\
n\partial_t \boldsymbol{U} + n\boldsymbol{U}\cdot\boldsymbol{\nabla}\boldsymbol{U} + \boldsymbol{\nabla} p = \boxed{q_h n_h \boldsymbol{E}^*} + \left(\dfrac{\boldsymbol{\nabla}\times\boldsymbol{B}}{\mu_0} - \boxed{q_h n_h \boldsymbol{U}_h}\right)\times\boldsymbol{B},\\
\partial_t p + \boldsymbol{\nabla}\cdot(p\boldsymbol{U}) + (\gamma-1)\,p\boldsymbol{\nabla}\cdot\boldsymbol{U} = 0,\\
\boldsymbol{E}^* = \boldsymbol{E} - \eta\boldsymbol{j} = -\boldsymbol{U}\times\boldsymbol{B}\\
\partial_t \boldsymbol{B} = -\boldsymbol{\nabla}\times\boldsymbol{E},
\end{array}
\right.
$$

..

$$
\left\{
\begin{array}{l}
\partial_t f_h + \boldsymbol{v}\cdot\boldsymbol{\nabla} f_h + \dfrac{q_h}{m_h}\left(\boldsymbol{E}^* + \boldsymbol{v}\times\boldsymbol{B}\right)\cdot\boldsymbol{\nabla}_v f_h = 0.\\
\boxed{n_h = \int f_h d^3v,}\quad \boxed{n_h\boldsymbol{u}_h = \int f_h v d^3 v.}
\end{array}
\right.
$$

Alfven wave destabilized by tenuous ion beam

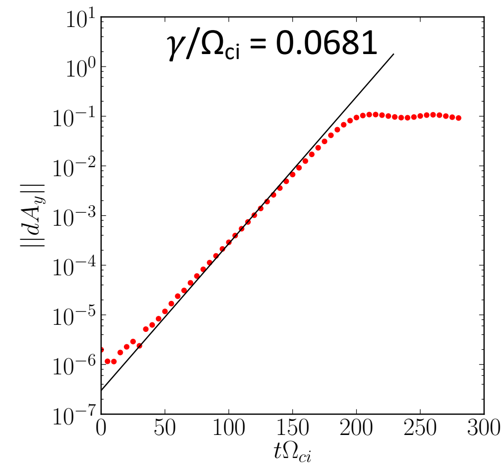

B= 1. $q_{beam} = m_{beam} = 1$, $n_{beam}/n = 0.05$, $v_{th,beam} = v_A$, $v_{0,beam} = 2.5\ v_A$

Los Alamos NATIONAL LABORATORY

6. Hands-on session

Hybrid-VPIC

VPIC (Vector Particle-In-Cell) code originally developed by K. Bowers (Bowers et al., Physics of Plasmas, 2008) has been used for some of the largest 3D PIC simulations performed:

- E.g. 10 trillion particles and 10 billion cells.
- VPIC philosophy: Simple algorithms that scale and run extremely fast.

"Hybrid-VPIC": New version implementing the quasi-neutral hybrid model:

- "Single pass" algorithm of H3D: Leapfrog particles, RK4 field-solve.

https://doi.org/10.1063/5.0146529

- Primary developer: Ari Le (Los Alamos National Laboratory).
- Open source:
  https://github.com/lanl/vpic-kokkos/tree/hybridVPIC
- Vlasov-Maxwell PIC: https://github.com/lanl/vpic
  https://github.com/lanl/vpic-kokkos

Hybrid-VPIC best practices

- For each simulation create a new folder in “scratch” (/ptmp/mpXX/folder) to run from.
- Build input deck against source every time changes are made “make”.
- Beware of dumping particle data: Can use massive amount of disk-space.
- In case of error, check log file e.g. “vpic.out”.
- Some things to try:
    - Decrease timestep.
    - Increase (or decrease) dissipation, e.g. hyper-resistivity.
- Contact: stanier@lanl.gov for questions/issues/bug reporting.
- Warning: Recently open sourced - check github for bug fixes! (and new features).

Proton Cyclotron Anisotropy Instability (PCAI)

- Electromagnetic instability driven by $P_{p\perp} > P_{p\parallel}$.

- Left hand polarization with resonant ions.
- Fastest growing mode has kxB = 0.

- Instability threshold:

$$\frac{P_\perp}{P_\parallel} - 1 \approx \frac{S}{\beta_{p\parallel}^{0.4}} \text{ with } S \sim 1.$$

  - Collisionless wave-particle scattering reduces $P_\perp / P_\parallel$ until saturation.

Gary, S. P. (1993). *Theory of space plasma microinstabilities* (No. 7). Cambridge university press.

PCAI input deck

1. Running and postprocessing data (see pcai/README).
   - cd pcai
   - emacs –nw pcai.cxx
   - make
   - sbatch subslurm
   - ftn –o translate_pcai translate_pcai.f90
   - mkdir data
   - ./translate_pcai
   - python ./plotsPCAI.py

2. Nominal simulation parameters:

$$\beta_{p\|} = 1, \ \frac{T_{p\perp}}{T_{p\|}} = 3, \ \frac{L_x}{d_i} = 10.5, \ \frac{T_e}{T_{p\|}} = 1, \ \gamma = \frac{5}{3}.$$

3. Numerical parameters:
   - 1D simulation, 64 cells, 10K particles/cell, $\Delta t\ \Omega_{ci}$ = 0.01, dissipation=0.

PCAI results for nominal parameters

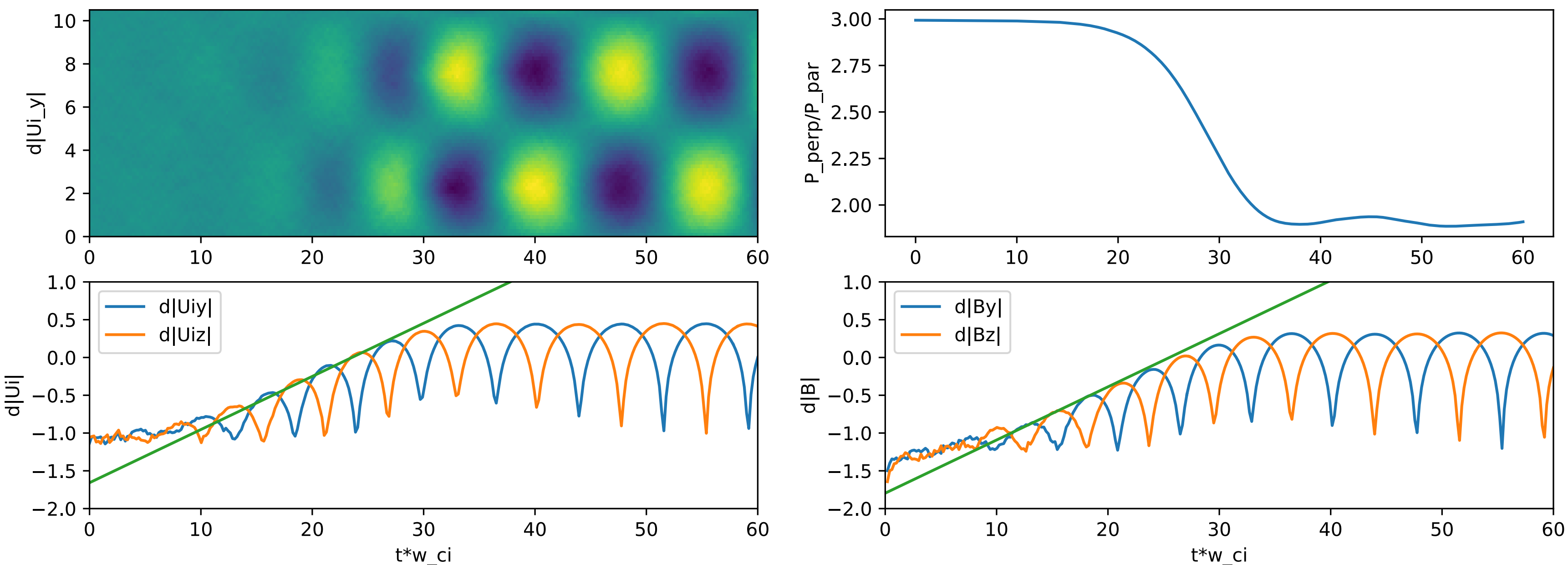

- Transverse velocity and magnetic field components grow from noise (LH Alfven waves).
- Agree with linear theory for these parameters (γ/Ω_{ci}=0.162).
- Pressure anisotropy decreases until saturation.

PCAI: Suggested exercises

- Compute growth rates across a range of beta & anisotropy.
  - Compare against linear solver. E.g. "HYDROS" by D. Told (New Journal Physics, 2016 - https://github.com/dtold/HYDROS).

- Advanced: Add a 20% density fraction of a minor species of alpha particles and find how this modifies the growth rate.
  - For parameters and results, see: Stanier, A., et al. (2019). A fully implicit, conservative, non-linear, electromagnetic hybrid particle-ion/fluid-electron algorithm. *Journal of Computational Physics*, *376*, 597-616.

Landau Damped Ion Acoustic Wave

- Fundamental electrostatic mode in hybrid-PIC model: Ion Acoustic Wave.
  - Driven by pressure perturbation.

  - Fluid models (e.g. Hall-MHD): wave is undamped.
  - Hybrid-PIC: Landau resonance damps the wave & locally flattens ion VDF (analogous to electron LD of Langmir waves).

  - Dispersion relation:

Plasma dispersion function

$$\frac{dZ(\zeta)}{d\zeta} = 2\tau, \quad \zeta \equiv (\omega - i\gamma)\,/kv_{\mathrm{th,i}}$$

T_i/T_e

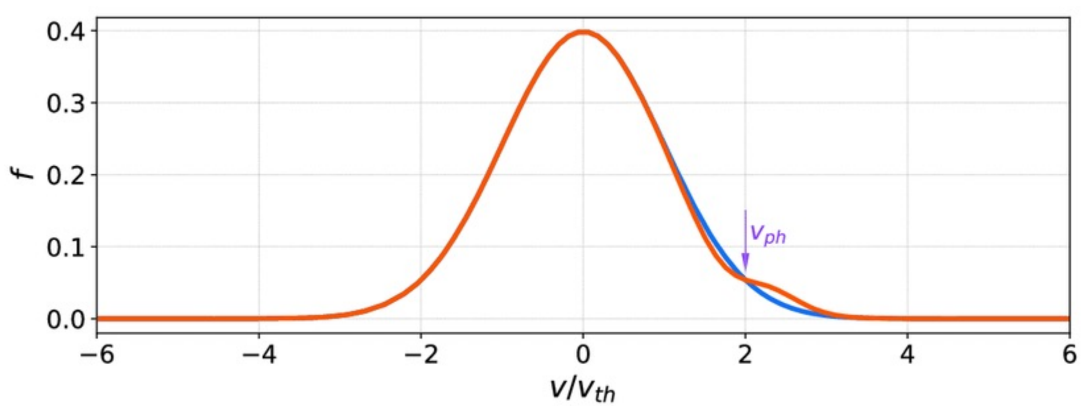

IAW input deck

1. Running and postprocessing data (see iaw/README).
   - cd iaw
   - emacs –nw iaw.cxx
   - make
   - sbatch subslurm
   - ftn –o translateIAW translateIAW.f90
   - mkdir data
   - srun –n 1 ./translateIAW
   - python ./plotsIAW.py

2. Nominal simulation parameters:

$$T_i = 1/3, \quad \gamma = 5/3, \quad c_s = \sqrt{\gamma T_e/m_i} = 1, \quad k_x = \pi/8, \quad \delta n = 2 \times 10^{-2}$$

3. Numerical parameters:
   - 1D simulation, 48 cells, 150K particles/cell !, $\Delta t = 0.02$, dissipation = 0.

Landau-damped IAW results for nominal parameters

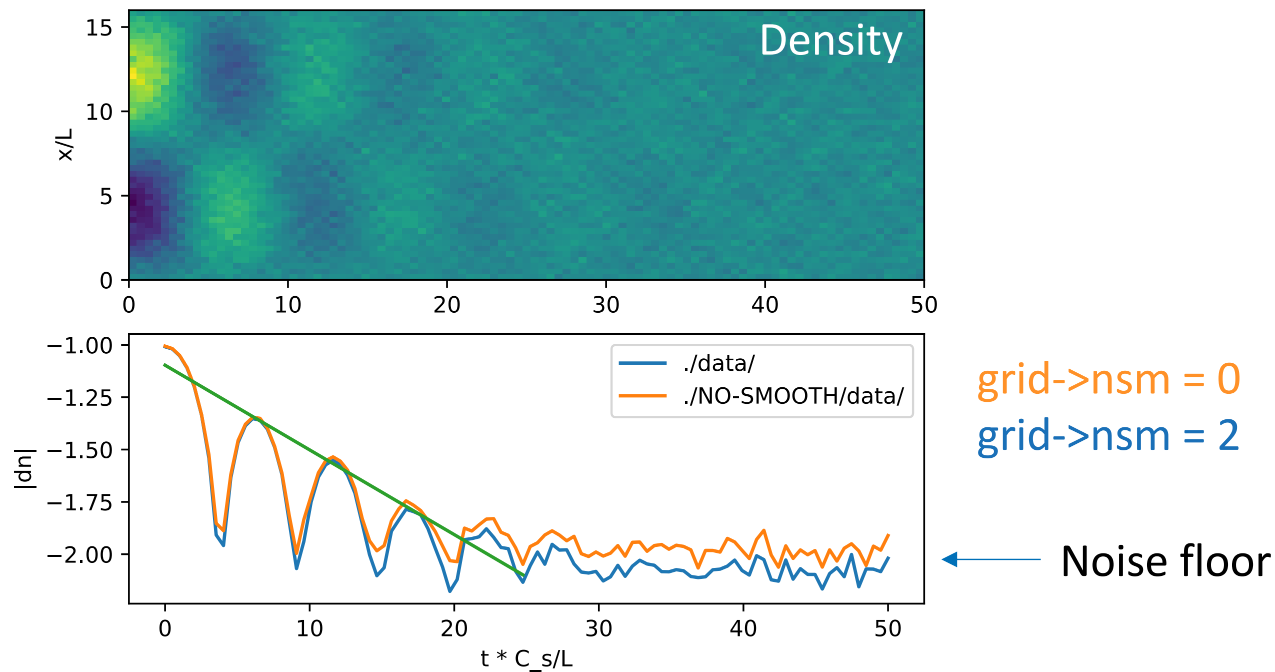

- Damping rate: γ = -0.0932.
- Initial perturbation damps to noise floor. Noise can be reduced by:
  1. Use more particles/cell (noise ~ 1/sqrt(N_p)).
  2. Binomial smoothing/higher order shape functions (see figure).
  3. Using low-discrepancy quasi-Random numbers to seed particles (noise ~ 1/N_p).
  4. Most efficient: Delta-F

Landau-damped IAW: Suggested further exercises

- See how temperature ratio T_i/T_e influences damping rate.

- What happens when we set T_i -> 0? (Finite grid unstable).
  - How is this the numerical instability threshold influenced by binomial smoothing?

- What happens when we use a larger perturbation? E.g. dn = 0.5?:
  - Non-linear Landau damping (phase space vortex structure).

Magnetic reconnection island coalescence

- Magnetic islands 2D versions of flux-ropes.
- Self-driven reconnection problem:
  - Coupling of ideal island motion to micro-scale reconnection physics.
  - Ion kinetic effects are crucial.
- Unstable Fadeev island equilibrium:
  - Magnetic field: $\boldsymbol{B} = \boldsymbol{\nabla} \times \boldsymbol{A}$

$$A_y = -\lambda B_0 \ln\left[\cosh\left(z/\lambda\right) + \epsilon \cos\left(x/\lambda\right)\right],$$

  - Density:

$$n = n_0(1-\epsilon^2)/\left[\cosh\left(z/\lambda\right) + \epsilon\cos\left(x/\lambda\right)\right]^2 + n_b$$

- Pressure balance: $\beta = \dfrac{2\mu_0 n_0 k_B\left(T_{i0} + T_{e0}\right)}{B_0^2} = 1$

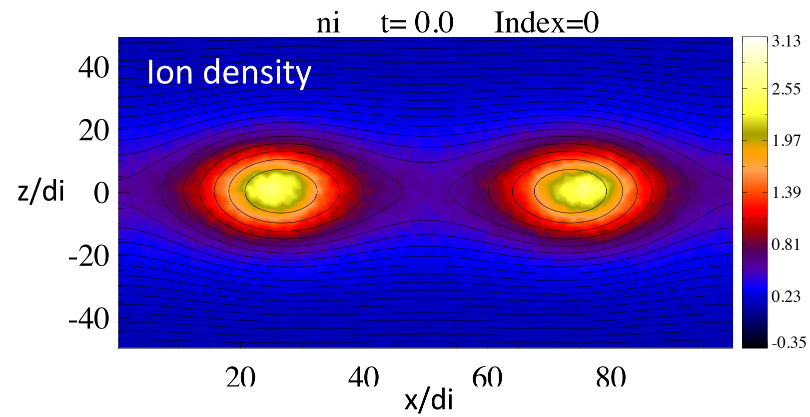

Island coalescence: input deck

1. Running and postprocessing data.
   - cd islands
   - emacs –nw islands.cxx
   - make
   - sbatch subslurm
   - ftn –o translate_islands translate_islands.f90
   - mkdir data
   - srun –n 1 ./translate_islands
   - ftn –o ayprog ay_gda_integrate.f90
   - ./ayprog
   - IDL gui: “module load idl” “idl” “diagnostic”. Python: “mkdir figs” “python plotfigs.py”.
   - “python ./rate.py”, “python opoint.py”.
2. Nominal simulation parameters:

$$\lambda = 5d_i, \quad \epsilon = 0.4, \quad n_b = 0.2n_0, \quad T_i/T_e = 1, \quad \eta = 10^{-3}, \quad \eta_H = 5 \times 10^{-3}, \quad \gamma = 1$$

3. Numerical parameters:
   - 2D simulation, 256x128 cells, 50 particles/cell, $\Delta t^*\Omega_{ci}$ = 0.005.

Los Alamos NATIONAL LABORATORY

Island coalescence problem: Results

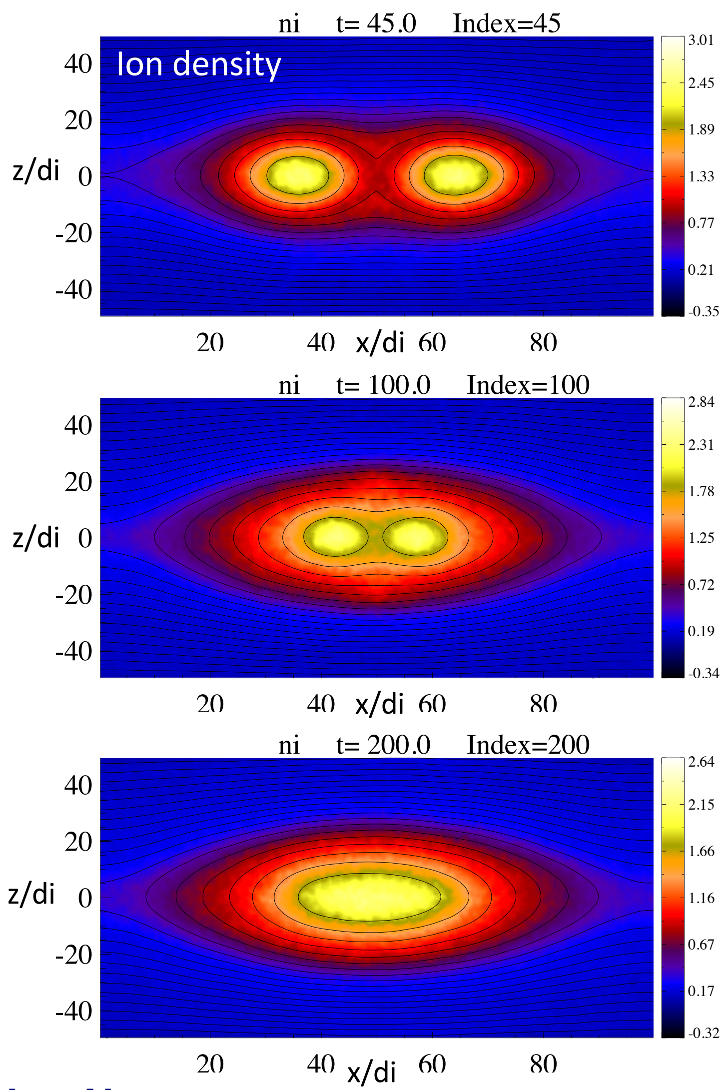

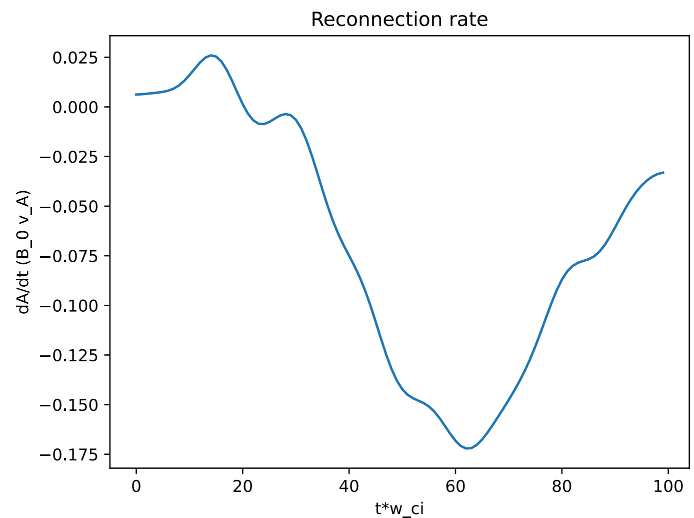

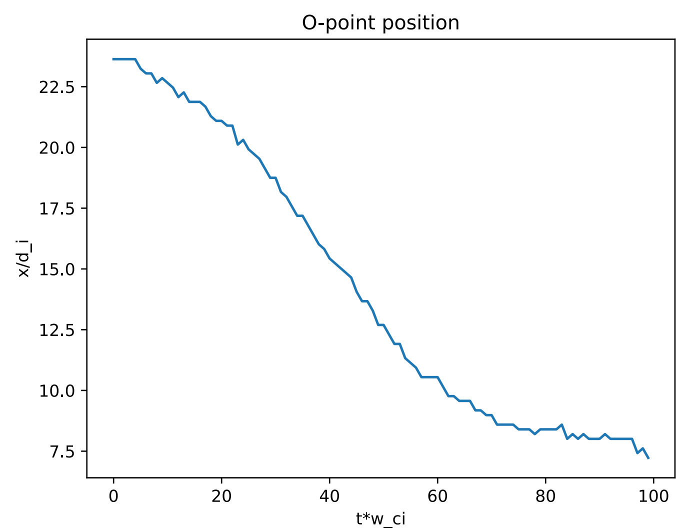

Island coalescence problem: Suggested exercises

- For these: Increase: resolution & particles/cell. Decrease: dissipation & timestep.

1. Vary ratio of Ti/Te and see how this modifies the reconnection rate and O-point motion (see Stanier et al., ”Role of ion kinetic physics in the interaction of magnetic flux ropes”, Phys. Rev. Lett. (2015)).

2. How does the addition of a “guide" field change the structure of the diffusion region and the reconnection rate? (see Stanier et al., ”The role of guide-field in magnetic reconnection driven by island coalescence”, Phys. Plasmas (2017)).

3. How do the maximum and average (merge time) rates of magnetic reconnection scale with the size of the islands (increasing λ/d_i).

Collisionless shock

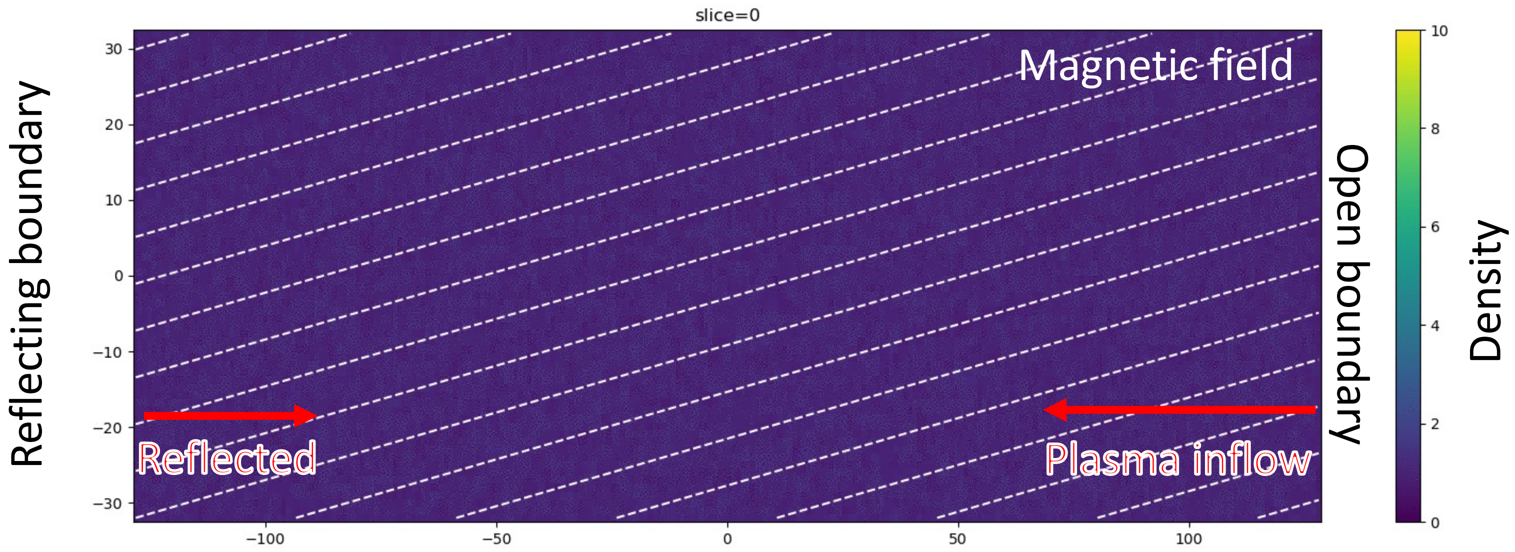

<u>2D magnetospheric shock problem:</u>

- M_A = 11.4 injected from right (open) boundary.
- Reflects from left boundary to drive collisionless shock.

Thank you for your attention!

Advertisement: LANL Space Weather Summer School

- Flyer from 2023.
- Next summer school in 2025 – look out for announcements.
- Deadline for applications usually in January.

Advertisement: Post-doc position in applied mathematics and plasma physics

Algorithm development:

- Low-noise particle-in-cell methods,
- low-rank methods,
- hybrid fluid-kinetic methods.

For applications of:

- Space weather,
- Magnetic confinement fusion,
- Inertial confinement fusion.

Apply at: https://lanl.jobs/Search/JobDetails/postdoctoral-researcher-in-applied-mathematics--plasma-physics (email stanier@lanl.gov for details).

LANL postdoc program:
https://collaboration.lanl.gov/postdoctoral-research/